Energy, Mass, Time, Space

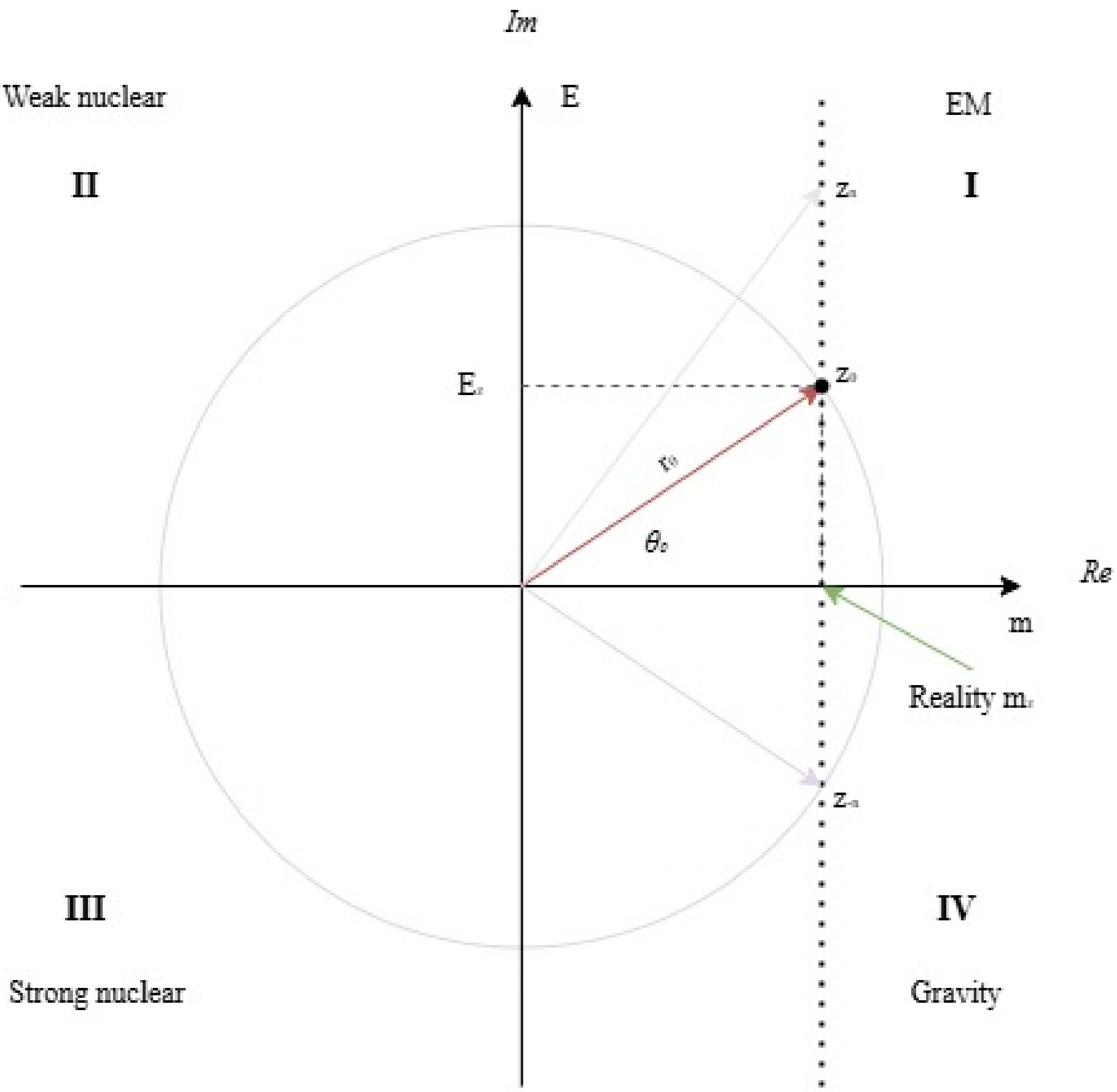

Compiled on January 11, 2026

To life.

Contents

License

Preface

In scientific discovery, pure mathematics often serves as the bedrock of our understanding of the universe. This essay is my attempt to develop, in real time with AI, an idea that has echoed in my mind for years. It is a perspective, not a declaration, and simply asks, *what if?*

> Don't think it doesn't make sense; ask yourself what sense it could have.

First, a mathematical framework is defined that ties Energy, Mass, Time and Space (EMTS), then speculates how the framework could fit with our knowledge.

Giancarlo Trevisan

Visualize then Realize!

Part I

Foundations

Chapter 1

The Complex Plane

The connection between the complex plane and reality becomes especially significant when we consider the origins and applications of imaginary numbers. Historically, the introduction of imaginary numbers emerged from attempts to solve cubic equations, as first systematically explored by Gerolamo Cardano in the 16th century. Cardano discovered that even when all solutions to a cubic equation were real, the algebraic process sometimes required passing through intermediate steps involving the square roots of negative numbers—quantities that had no clear interpretation at the time.

This mathematical curiosity turned out to be much more than a formal trick. The development of complex numbers enabled mathematicians and physicists to describe phenomena that could not be captured by real numbers alone. A profound example is the discovery of electromagnetic waves. In the 19th century, James Clerk Maxwell formulated his famous equations, which describe how electric and magnetic fields propagate and interact. The solutions to Maxwell's equations are most naturally expressed using complex exponentials, where the imaginary unit i encodes oscillatory behavior—essential for describing wave phenomena such as light and radio waves (see Maxwell's equations[**?**]).

Thus, imaginary numbers are not merely abstract constructs; they are indispensable tools for modeling and understanding the physical world. Their use reveals that reality possesses layers and symmetries that extend beyond direct sensory perception, hinting at a deeper mathematical structure underlying the universe. The complex plane, therefore, is not just a mathematical convenience but a window into the hidden fabric of nature.

The complex plane, a mathematical construct that allows us to visualize complex numbers as points in a two-dimensional space. In this plane, the horizontal axis represents the real numbers, while the vertical axis represents the imaginary numbers. For our purposes, we will map mass onto the real axis and energy onto the imaginary axis. Why this choice? Well, mass seems more real than energy from my point of view (feel free to swap). With this picture in mind, let's pick a point z_0 on the complex plane and dive into its possible implications.

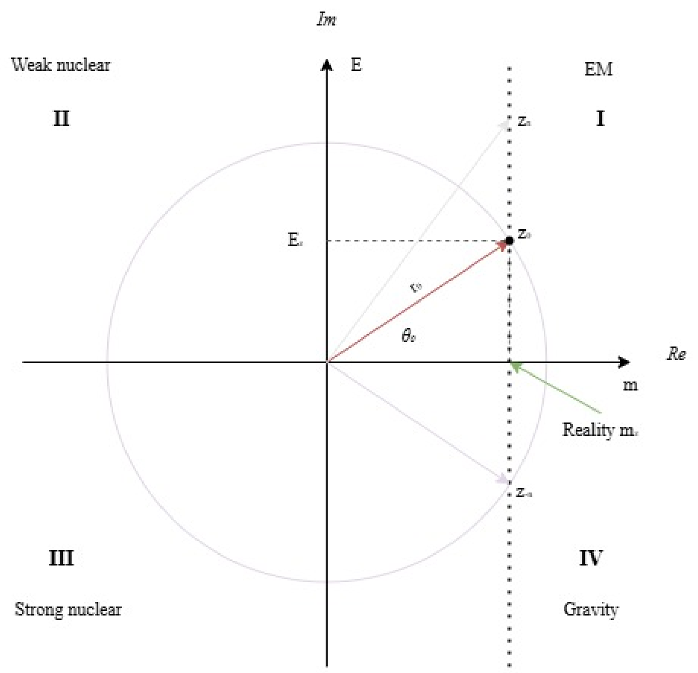

Figure 1.1: Complex plane illustration. m_z is what we perceive at time θ_0 and space r_0.

Chapter 2

The EMTS Framework: Core Definitions

Having introduced the complex plane and its historical significance, we now establish the foundational elements of the Energy-Mass-Time-Space (EMTS) framework. This chapter consolidates the core mathematical definitions and physical interpretations that underpin the entire theory.

2.1 The complex plane mapping

The EMTS framework posits that physical states can be represented as points in the complex plane:

$$z = m + iE,$$

where:

- m is the mass component (mapped to the real axis)
- E is the energy component (mapped to the imaginary axis)
- $i = \sqrt{-1}$ is the imaginary unit

This choice reflects the intuition that mass is "more tangible" than energy in everyday experience, though the mapping could be reversed without loss of generality. What matters is the *relationship* between the components, not which axis they occupy.

2.2 Polar representation

Every complex point z can be expressed in polar form:

$$z = re^{i\theta} = r(\cos\theta + i\sin\theta),$$

where:

- $r = |z| = \sqrt{m^2 + E^2}$ is the **modulus** (unified magnitude)
- $\theta = \arg(z) = \arctan(E/m)$ is the **argument** (unified phase)

2.2.1 Physical interpretation of r and θ

The modulus r represents the total mass-energy content:

$$r = \sqrt{(mc^2)^2 + E^2} \quad \text{or in natural units} \quad r = \sqrt{m^2 + E^2}.$$

The argument θ encodes the **partition** between mass and energy:

$$m = r\cos\theta, \tag{2.1}$$
$$E = r\sin\theta. \tag{2.2}$$

Crucially, we identify θ with time evolution:

$$\theta(t) = \omega t,$$

where ω is the angular frequency related to energy by $E = \hbar\omega$ (Planck's quantum hypothesis).

2.2.2 The projection principle

Central postulate: Physical reality corresponds to the *projection* of the complex state onto the real axis:

$$\text{Observable reality} = \Re(z) = m = r\cos\theta.$$

This projection is **many-to-one**: infinitely many complex states

$$\{z_n = m + iE_n\}_n$$

all project to the same observable value m. The imaginary component E represents hidden degrees of freedom that influence dynamics but are not directly observed.

2.3 Fundamental relationships

2.3.1 Time as phase

The identification $\theta = \omega t$ unifies time evolution with rotation in the complex plane. A state evolves as:

$$z(t) = re^{i\omega t}.$$

The observable projection oscillates:

$$m(t) = r\cos(\omega t),$$

explaining wave-like behavior from the geometry of rotation.

2.3.2 Energy-frequency connection

From quantum mechanics:

$$E = \hbar\omega \quad \Rightarrow \quad \omega = \frac{E}{\hbar}.$$

Thus the rotation rate in the complex plane is proportional to energy, linking dynamics to the imaginary component.

2.3.3 Measurement and collapse

In standard quantum mechanics, measurement "collapses" the wavefunction. In the EMTS framework:

1. Before measurement: Full state is $z = m + iE$ with complex dynamics
2. Measurement: Projects to $\Re(z) = m$
3. After measurement: The imaginary component E remains but is decohered from the observable m

Multiple branches with different E values persist along the imaginary axis (see Chapter 7 for the multiverse interpretation).

2.4 Force quadrants

The complex plane is divided into four quadrants based on the sign of m and E. We hypothesize that fundamental forces correspond to phase windows:

Quadrant	Force	Phase Range	Symbol
I	Electromagnetic	$0 < \theta < \frac{\pi}{2}$	Q_{I}
II	Weak	$\frac{\pi}{2} < \theta < \pi$	Q_{II}
III	Strong	$\pi < \theta < \frac{3\pi}{2}$	Q_{III}
IV	Gravitational	$\frac{3\pi}{2} < \theta < 2\pi$	Q_{IV}

Each force is characterized by a phase window $W_f(\theta)$ and coupling function $g_f(\theta, r)$. The observed interaction strength depends on where the state $z(t)$ resides in the phase cycle (see Chapter 5 for details).

2.5 Notation conventions

Throughout this work, we use the following notation:

- $z = m + iE = re^{i\theta}$ — Complex state (canonical form: $z = m + iE = re^{i\theta}$)
- $\theta = \omega t$ — Phase-time relation (shorthand: $\theta = \omega t$)
- $r = |z|$ — Modulus (total mass-energy)
- $\Re(z) = r\cos\theta = r\cos\theta$ — Real projection (observable)
- $\Psi(z, t)$ or $\Psi(r, \theta)$ — Wavefunction on complex state space
- $Q_{\text{I}}, Q_{\text{II}}, Q_{\text{III}}, Q_{\text{IV}}$ — Force quadrants (EM, Weak, Strong, Gravitational)

2.6 Relationship to standard physics

The EMTS framework is not a replacement for quantum mechanics or relativity, but a *geometric reinterpretation* that:

- Recovers the Schrödinger equation in appropriate limits
- Naturally incorporates special relativity through $r = \sqrt{m^2 + E^2}$
- Provides a unified language for discussing particles, forces, and spacetime
- Suggests extensions (e.g., multiverse structure, dark matter) that emerge from the geometry

Standard formulations are recovered by:

1. Restricting to the real axis (classical limit)
2. Quantizing the phase θ (quantum mechanics)
3. Coupling the modulus r to spacetime curvature (general relativity)

2.7 Summary: The EMTS postulates

We summarize the core framework:

1. **Complex representation**: Physical states are complex numbers $z = m + iE$
2. **Polar dynamics**: States evolve as $z(t) = re^{i\omega t}$ with $\omega = E/\hbar$
3. **Projection principle**: Observable reality is $\Re(z)$; imaginary components are hidden
4. **Phase-force mapping**: Forces correspond to phase windows in $[0, 2\pi)$
5. **Quantization**: Periodicity in θ leads to discrete spectra
6. **Dimensionality from precision**: Effective dimensionality increases with measurement precision

The remaining chapters develop these postulates in detail, exploring their implications for quantum mechanics (Part I), the Standard Model (Part II), specific phenomena (Part III), and future directions (Part IV).

Chapter 3

Polar Representation and Its Implications

Building on the core framework (Chapter 2), we explore deeper implications of the polar representation $z = m + iE = re^{i\theta}$. This chapter examines how the modulus r and argument θ relate to physical measurements and quantum phenomena.

3.1 Extended physical interpretation

The modulus and argument were defined in the core framework as:

$$r = \sqrt{m^2 + E^2}, \qquad \theta = \arctan\left(\frac{E}{m}\right).$$

In units where $c = 1$, or more generally $r = \sqrt{(mc^2)^2 + E^2}$ and $\theta = \arctan(E/mc^2)$.

Space and Time. The key relation $\theta = \omega t$ with $E = \hbar\omega$ means probabilities or densities linked to projections oscillate with ω. The projection $m_z = \Re(z) = r\cos\theta$ can repeat with period 2π even as the underlying phase history differs.

Projection as Measurement. With the unit vector $|\psi\rangle = \cos\theta\,|m\rangle + i\sin\theta\,|E\rangle$, a mass measurement uses P_m and yields $\mathbb{P}(m) = \cos^2\theta$, mirroring $m_z = r\cos\theta$. Standard treatments of such two-level mappings can be found in Griffiths[**?**].

Chapter 4

Hermitian Operators on a Hilbert Space

Let $H = \mathbb{C}^2$ with basis $\{|m\rangle, |E\rangle\}$. A normalized state is

$$|\psi\rangle = \cos\theta\,|m\rangle + i\sin\theta\,|E\rangle, \qquad \langle\psi|\psi\rangle = 1.$$

Observables A are Hermitian with spectral decomposition $A = \sum_k a_k P_k$. Measurement of a_k occurs with probability $\langle\psi|P_k|\psi\rangle$ and the post-measurement state is $P_k|\psi\rangle/\sqrt{\langle\psi|P_k|\psi\rangle}$.

For a "mass" measurement, $P_m = |m\rangle\langle m|$, so $\mathbb{P}(m) = \cos^2\theta$, echoing the geometric projection $\Re(z) = r\cos\theta$.

Unitary evolution with $H = \frac{\hbar\omega}{2}\sigma_y$ yields $\mathbb{P}(m,t) = \cos^2(\omega t)$, bridging to $\theta = \omega t$.[**?**]

Chapter 5

The Quadrants and Their Implications

Let the pre-measurement state be $z(t_0) = re^{i\theta_0}$. A projection onto the real axis yields $m_z = r\cos\theta$. Hypothesis: the interaction channel observed in spacetime is tagged by the pre-collapse quadrant of $z(t_0)$.

- Quadrant I (Q_{I}, $0 < \theta_0 < \frac{\pi}{2}$): Electromagnetic
- Quadrant II (Q_{II}, $\frac{\pi}{2} < \theta_0 < \pi$): Weak
- Quadrant III (Q_{III}, $\pi < \theta_0 < \frac{3\pi}{2}$): Strong
- Quadrant IV (Q_{IV}, $\frac{3\pi}{2} < \theta_0 < 2\pi$): Gravitational

With phase windows $W_f(\theta)$ and coupling $g(\theta, r)$, a cycle-averaged strength at radius r is

$$\bar{g}_f(r) = \frac{\omega(r)}{2\pi} \int_0^{2\pi} W_f(\theta)\, g(\theta, r)\, d\theta.$$

Part II

Framework and Mechanics

Chapter 6

Standard Model

Building on the EMTS framework (Chapter 2), we map Standard Model particles and forces onto the complex plane. In quantum theory, the state encodes probabilities.[?] In this framework, oscillations with frequency ω link to detection likelihoods. Particle vs. wave is reconciled: coherent evolution (*wave*) sets channel rates, while projection events (*particles*) are localized outcomes.

Particle vs. Wave

- **State vector**: carries phase and interferes.
- **Measurement**: projects to outcomes with Born probabilities.
- **Field view**: particles are quantized excitations; waves are coherent field amplitudes.

With $z(t) = re^{i\omega t}$ and windows $W_f(\theta)$ from Chapter 5, a minimal rate model is

$$R_f(r) = \frac{\omega}{2\pi} \int_0^{2\pi} W_f(\theta)\, g(\theta, r)\, d\theta.$$

Quarks in the complex plane

In the EMTS picture we write a generic excitation as $z = m + iE = re^{i\theta}$, with r encoding a space-like scale and $\theta = \omega t$ encoding time-like phase. Quarks can be viewed as excitations whose complex-plane behaviour is constrained by threefold structure:

- **Colour charge** corresponds to how the excitation winds in an internal copy of the complex plane, with three preferred phase orientations ("red, green, blue") in an $SU(3)$-like subspace.
- **Confinement** arises because a single quark's complex trajectory cannot close in the observable m–E plane; only colour-neutral combinations lead to closed orbits and stable projections.
- **Flavour** (up, down, strange, etc.) is tied to distinct radii r and characteristic angular frequencies ω, leading to different effective masses and couplings.

In this view, quarks occupy specific bands in r and families of allowed phase patterns in θ, with hadrons emerging as composite closed paths whose joint projection appears as a single particle.

Leptons as simpler orbits

Leptons lack colour charge and so correspond to simpler trajectories on the same complex plane. Their key properties emerge from how their paths relate to the real and imaginary axes:

- **Charged leptons** (electron, muon, tau) follow orbits with a nonzero average real projection $\langle m_z \rangle$, giving rest mass, while their interaction with the electromagnetic field shifts θ and modulates E.
- **Neutrinos** are nearly lightlike: their trajectories lie close to the imaginary axis, with very small m but nontrivial phase evolution, which can support flavour oscillations as slow precessions between nearby orbits.
- **Generations** correspond to nested shells in r with similar angular patterns but different characteristic frequencies, reflecting the mass hierarchy without changing the basic complex geometry.

Leptons thus occupy cleaner, less composite regions of the complex plane, making them ideal probes of how m and E trade off along a single worldline.

Forces as phase symmetries

Forces in the Standard Model act by reshaping or constraining motion on the complex plane rather than by pushing in ordinary space alone. We can sketch them as follows:

- **Electromagnetism** tracks changes in the global phase of charged trajectories. A $U(1)$ gauge transformation is a shift $\theta \mapsto \theta + \alpha$, leaving r fixed but altering interference patterns and detection rates.
- **Weak interactions** mix components of z associated with different leptonic and quark flavours. Geometrically this can be pictured as rotations between nearby orbits in a multi-dimensional complex space, with massive gauge bosons mediating large, localized phase jumps.
- **Strong interactions** constrain colour phases so that only colour-neutral combinations yield closed, low-action paths. Gluon exchange continually rewires how individual quark trajectories share a joint complex-phase structure inside hadrons.

All three gauge forces can be summarised as rules about which deformations of the complex trajectory $z(t)$ leave physical rates invariant and which cost action, echoing the role of symmetries and gauge fields in the usual Standard Model.

A unified placement

In summary, the complex plane provides a common stage:

- **Quarks** occupy structured, colour-charged orbits whose composites form closed, observable paths.
- **Leptons** trace cleaner, single-particle trajectories distinguished mainly by radius and frequency.

- **Forces** appear as symmetries and constraints on allowed deformations of these complex paths.

This speculative mapping does not replace the field-theoretic Standard Model,[**?**] but it offers a geometric intuition: all fundamental matter and forces inhabit different patterns of motion and symmetry on an underlying complex m–E plane.

Chapter 7

Mapping Reality

7.1 Reality as projection

Recall from the core framework (Chapter 2) that physical states are represented as $z = m + iE = re^{i\theta}$, where r is the total mass-energy magnitude and θ is the phase encoding the partition between mass and energy components.

Reality emerges as the projection of the complex plane onto the real axis. For any complex state $z = a + ib$, what we observe—what we call "reality"—is the real component a. This projection is many-to-one: an infinite number of complex points

$$z_n = a + ib_n, \quad n \in \mathbb{Z} \text{ or } \mathbb{R},$$

all project to the same real value a. Each distinct imaginary component b_n represents a different hidden state, a different branch of possibility, yet all manifest identically in observable reality.

This degeneracy is profound: what appears as a single measurement outcome in our three-dimensional reality corresponds to an entire vertical line in the complex plane. The vast multiplicity of states "behind" each observation hints at the richness of the underlying structure.

7.2 Precision, dimensionality, and quantization

Conventional physics treats space and time as continuous manifolds with fixed dimensionality (3+1). The EMTS framework suggests a more subtle picture: **dimensionality is conveyed by precision**.

Consider a spatial coordinate x. At low precision (coarse-grained measurement), x appears one-dimensional. As we increase precision, we resolve finer structure:

- At scale Δx_1, position is a single real number
- At scale $\Delta x_2 \ll \Delta x_1$, we resolve additional degrees of freedom: $x = x_{\text{coarse}} + \delta x$
- At Planck scale $\Delta x_P \sim 10^{-35}$ m, quantum geometry emerges, revealing discrete structure

The apparent dimensionality D_{eff} grows with precision ϵ:

$$D_{\text{eff}}(\epsilon) \sim D_0 + \alpha \log\left(\frac{L_{\max}}{\epsilon}\right),$$

where D_0 is the macroscopic dimension, $L_{\max}$ is the largest accessible scale, and α encodes how complexity unfolds at finer scales.

Similarly for time: what appears as a single temporal coordinate t at macroscopic precision becomes a rich structure at finer scales, potentially revealing branching, quantization, or phase-dependent flow rates (as encoded in $\mathcal{N}(x, \rho)$ from the unified framework).

7.3 Quantization and the multiverse

The projection degeneracy, combined with precision-dependent dimensionality, naturally leads to a **quantized multiverse structure**.

At each "point" in observable reality a, there exists a discrete (quantized) or continuous tower of states parameterized by the imaginary axis:

$$\{z_n = a + ib_n\}_n.$$

The quantization arises from the periodic structure in θ. Recall that physical states satisfy

$$\Psi(r, \theta + 2\pi) = \Psi(r, \theta),$$

leading to quantized phase modes:

$$\Psi_n(r, \theta) = R_n(r)\, e^{in\theta}, \quad n \in \mathbb{Z}.$$

Each integer n labels a different "branch" or "universe" characterized by:

- Winding number n around the origin in the complex plane
- Distinct energy spectrum from the Hamiltonian $\hat{H}_\theta = -\frac{\hbar^2}{2I_\theta}\partial_\theta^2 + U_{\text{quad}}(\theta)$
- Different coupling strengths to gauge forces via sector projectors $P_s(\theta)$

7.3.1 Many-worlds from many-phases

When a measurement occurs, the projection $z \to \text{Re}(z)$ collapses an infinite-dimensional phase space to a single real outcome. But the framework suggests that **all branches persist in the imaginary direction**. What appears as "wavefunction collapse" in conventional quantum mechanics is simply:

1. Projection: $z = a + ib \to a$ (observable outcome)
2. Persistence: The full state $z = a + ib$ continues to evolve
3. Branching: Different values of b (or equivalently θ) represent parallel realities, all projecting to the same a at the moment of measurement

The multiverse is not a set of disconnected universes, but rather a **continuum of phase-shifted realities**, all coexisting along the imaginary axis, distinguishable only by their internal phase structure θ, which determines:

- Which force quadrant dominates
- The rate of time flow via $\mathcal{N}(x, \rho, \theta)$
- Coupling to different gauge sectors
- Mass-energy partitioning via $\cos\theta$ and $\sin\theta$

7.3.2 Cross-branch interference

Although branches with different θ values project to the same real outcome, they can interfere quantum mechanically. The overlap integral

$$\mathcal{I}_{nm} = \int_0^{2\pi} d\theta\, \Psi_n^*(\theta)\, \hat{O}\, \Psi_m(\theta)$$

describes interference between branches n and m under observable $\hat{O}$. When $\mathcal{I}_{nm} \neq 0$, the branches are not fully independent—they constitute an entangled multiverse.

This framework recovers:

- **Decoherence:** Branches with $\Delta\theta \gg 1$ rapidly dephase, making $\mathcal{I}_{nm} \to 0$
- **Quantum superposition:** States with nearby θ values maintain coherence
- **Many-worlds interpretation:** Each θ-sector evolves independently when decoherence is complete

7.4 Implications for observers

An observer embedded in reality sees only the projection $\mathrm{Re}(z)$. The observer's consciousness, measurement apparatus, and memory all exist in this projected space. Yet the full state $z = a+ib$ evolves according to the complex dynamics.

This creates an epistemic horizon: we can infer the existence of the imaginary component through:

1. **Quantum interference:** The imaginary part influences the evolution of the real part
2. **Entanglement:** Correlations between spatially separated real projections reveal hidden phase structure
3. **Gravitational effects:** The magnitude $r = \sqrt{a^2 + b^2}$ affects spacetime curvature, even though we only observe a
4. **Statistical ensembles:** Repeated measurements probe the distribution over b, revealing the underlying complex structure

7.5 Reconciling continuity and discreteness

The framework unifies apparently contradictory aspects of quantum mechanics and general relativity:

Aspect	**Continuous**	**Discrete**
Space	Manifold $\mathcal{M}$	Precision-dependent $D_{\text{eff}}(\epsilon)$
Time	Parameter t	Clock rate $\mathcal{N}(x,\rho)$, phase θ
Phase	Circle S^1	Quantized modes $e^{in\theta}$
Energy	Spectrum of $\hat{H}$	Eigenvalues E_n
Multiverse	Continuum of θ	Branches labeled by $n \in \mathbb{Z}$

At macroscopic scales and low precision, continuity dominates. At microscopic scales and high precision, discreteness emerges. The transition is smooth, governed by the characteristic scales $\hbar$, c, and the phase inertia I_θ.

7.6 The projection principle

We formalize the central insight:

> *Physical reality is the real projection of a complex state space. Observable phenomena correspond to* $Re(z)$*, while the imaginary component* $Im(z)$ *encodes hidden degrees of freedom—phase structure, interaction potentials, and alternate branches. Measurement selects a real outcome from an infinite multiplicity of complex pre-images, each representing a distinct universe in the quantized multiverse.*

This projection principle explains:

- Why quantum mechanics is probabilistic (many z map to one a)
- Why entanglement is nonlocal (correlations exist in the imaginary direction)
- Why spacetime is dynamical (geometry responds to $|z|$, not just $\text{Re}(z)$)
- Why observers cannot access "other universes" directly (they live in the projection)
- Why precision matters (finer measurements probe finer structure in the complex plane)

Particles are points tracing oscillatory motion; forces emerge as structured relations across quadrants; spacetime geometry echoes these mathematical ties. But beneath it all lies a richer reality: a complex-valued ocean, of which we perceive only the surface.

Chapter 8

Quantum Properties on the Complex Plane

Quantum behaviour can be reframed in the EMTS picture established in Chapter 2. Recall that physical states are represented as $z = m + iE = re^{i\theta}$ with $\theta = \omega t$. Projection to the real axis $(r \cos \theta)$ encodes what is classically observed, while the full complex motion remains hidden but dynamically essential.

8.1 Wave–particle duality as rotating projection

Take a single point $z(t) = re^{i\omega t}$. The real projection

$$m_z(t) = \Re z(t) = r \cos \theta(t)$$

oscillates, while discrete detection events correspond to sampling m_z at particular θ and locations in r. The "wave" is the smooth, complex rotation; the "particle" is the localized real-axis readout.

When several paths $z_k(t)$ are allowed, they add in the complex plane before projection:

$$z_{\text{tot}}(t) = \sum_k z_k(t).$$

Interference patterns arise because $\Re z_{\text{tot}}$ depends on relative angles θ_k, not just moduli r_k, mirroring standard complex-amplitude interference from part2-framework-mechanics/standard-model.tex.

8.2 Superposition as geometric addition

A superposed state of two alternatives A and B becomes a vector sum

$$z = \alpha z_A + \beta z_B,$$

with $\alpha, \beta \in \mathbb{C}$ encoding weights and phases. Only after projection does one obtain an outcome associated with z_A or z_B, analogous to

$$|\psi\rangle = \cos \theta \, |m\rangle + i \sin \theta \, |E\rangle$$

in part1-foundations/hermitian-operators.tex. The angle between z_A and z_B in the plane governs constructive or destructive interference in $\Re z$, giving a geometric visualization of the Born rule.

8.3 Uncertainty as phase–projection complementarity

If reality is read off as the real projection $m_z = r\cos\theta$, then sharp knowledge of m_z constrains θ to narrow windows where m_z takes that value. Conversely, if θ is highly delocalized over $[0, 2\pi)$, many different m_z values are sampled.

Formally, treat θ as an angle on a circle and its conjugate as an integer winding number n (counting how many 2π cycles the phase accumulates). Angle–number pairs satisfy an uncertainty relation of the form

$$\Delta n\,\Delta\theta \gtrsim \tfrac{1}{2},$$

which mirrors $\Delta E\,\Delta t$ once E is tied to angular frequency via $E = \hbar\omega$. In EMTS, the spread in θ (time-like phase) and the spread in m_z (measured mass-like projection) are thus inherently linked, explaining why precise localization in one degrades certainty in the other.

8.4 Quantization from closed-orbit conditions

Quantization appears naturally if allowed states correspond to closed or resonant trajectories on the complex circle. Requiring that after an evolution period T the point returns to itself,

$$\theta(T) - \theta(0) = 2\pi n, \qquad n \in \mathbb{Z},$$

imposes discrete conditions on ω and hence on $E = \hbar\omega$. More generally, demanding single-valuedness of $\Psi(r, \theta)$ on S^1_θ—as in the phase space discussed in part4-future/theory-of-everything.tex—forces integer winding numbers and a tower of allowed modes. The complex circle then acts as a geometric origin for energy levels and other quantized spectra.

8.5 Entanglement as correlated complex geometry

For two subsystems A, B with points $z_A = r_A e^{i\theta_A}$ and $z_B = r_B e^{i\theta_B}$, an entangled state can be represented by a joint amplitude $\Psi(z_A, z_B)$ on the product of two complex planes, as developed in part3-implementation/entanglement.tex. A simple form,

$$\Psi(z_A, z_B) \propto e^{im(\theta_A - \theta_B)},$$

locks their phase difference while leaving the common angle free. Measurements project each point separately to the real axis, but correlations in outcomes reflect the underlying constraint on (θ_A, θ_B) and hence on (m_{z_A}, m_{z_B}).

In this view, entanglement is not mysterious action at a distance but a single geometric object on (z_A, z_B) space whose projections on separate real axes remain correlated even when r_A and r_B are widely separated.

8.6 Summary

Wave–particle duality, superposition, uncertainty, quantization, and entanglement all become features of how complex points move, add, and close on the EMTS plane, and how partial projections slice this richer geometry into the classical realities we observe.

Part III

Implementation

Chapter 9

Entanglement on the Complex Plane

9.1 Framing EMTS variables for entanglement

Recall from Chapter 2 that EMTS represents physical events as points on the complex plane $z = m + iE = re^{i\theta}$, with r encoding space and θ encoding time. Two-system entanglement can be modeled on pairs (z_A, z_B) by building joint states and correlators that respect EMTS' polar structure. In this view, time has two aspects: a monotone history variable (global θ-translation) and a periodic phase (modulo 2π), which naturally invites resonance phenomena and Floquet-like behavior in θ space.

9.2 A minimal mathematical insertion

9.2.1 State, reduction, and θ-symmetry

- **Global state:** Let $|\Psi\rangle$ live on a Hilbert space over EMTS points; for two subsystems A, B at $z_A = r_A e^{i\theta_A}$, $z_B = r_B e^{i\theta_B}$, write the joint amplitude $\Psi(z_A, z_B)$.[?]
- **Entanglement test:** Compute $\rho_A = \mathrm{Tr}_B\, |\Psi\rangle\langle\Psi|$ and a measure $S_A = -\mathrm{Tr}(\rho_A \log \rho_A)$ (or a negativity). Entanglement is present iff ρ_A is mixed.
- **θ-translation invariance:** If dynamics and initial conditions are invariant under simultaneous shifts $\theta_A \to \theta_A + \alpha$, $\theta_B \to \theta_B + \alpha$, then any entanglement measure depends only on the phase difference $\Delta\theta = \theta_A - \theta_B$ and the radii (r_A, r_B), not on absolute θ (stationarity):

$$\partial_\Theta S_A = 0, \quad \Theta = \tfrac{1}{2}(\theta_A + \theta_B).$$

9.2.2 Interaction kernels on the complex plane

- **Phase-sensitive coupling:**

$$H_{\text{int}} = \lambda\, f(r_A, r_B)\, \cos(\Delta\theta - \phi_0)\, \hat{O}_A \otimes \hat{O}_B,$$

  which entangles A and B when $f \neq 0$. The $\cos(\Delta\theta)$ factor makes phase relations explicit; ϕ_0 sets a preferred phase alignment.

- **Holomorphic form (optional):**

$$H_{\text{int}} = \lambda\, g(z_A, z_B)\, \hat{O}_A \otimes \hat{O}_B + \text{h.c.},$$

  with g holomorphic to ensure Cauchy–Riemann compatibility in EMTS. This yields entanglement protected along contours of constant argument or modulus depending on g.

9.3 Resonance as phase-locking in θ-time

- **Phase-locked entanglement:** If time has a periodic component, entanglement can strobe at resonant phase differences. With a drive of frequency ω on θ, stroboscopic evolution produces

$$U_F = e^{-iH_{\text{eff}}T}, \quad T = \tfrac{2\pi}{\omega},$$

and entanglement peaks when $\Delta\theta$ satisfies locking conditions (e.g., $\Delta\theta \approx \phi_0 \bmod 2\pi$).

- **Growth vs. invariance:** In generic (chaotic) dynamics, entanglement exhibits universal growth and saturation patterns (e.g., area-law to volume-law crossover with velocity v_E). "Entanglement is independent of time" can be realized when the initial state and generator are θ-stationary so only $\Delta\theta$ matters, or when a resonance creates steady phase-locking so the entanglement measure becomes θ-periodic and effectively constant under coarse graining.

9.4 Time independence and projection on the real axis

- **Projection choice matters:** If "projected on the real axis" means evaluating observables at fixed θ (equal-time slice), entanglement reduces to a function of radii and their separation along r, i.e., $S_A = S_A(r_A, r_B, \Delta\theta)$ with $\Delta\theta = 0$. With θ-translation invariance, this yields entanglement profiles depending only on spatial relations in r.

- **Integrating out θ:** Alternatively, integrating phases (or averaging over Θ) leaves phase-invariant correlators:

$$\overline{C}(r_A, r_B) = \frac{1}{2\pi}\int_0^{2\pi} d\Theta\; C\big(r_A e^{i(\Theta+\Delta\theta/2)},\, r_B e^{i(\Theta-\Delta\theta/2)}\big).$$

9.5 Testable consequences and a concrete ansatz

9.5.1 A simple EMTS entangled pair

$$\Psi(z_A, z_B) = \frac{1}{\sqrt{2}}\Big[\phi_0(r_A)\phi_1(r_B)\, e^{im(\theta_A-\theta_B)} + \phi_1(r_A)\phi_0(r_B)\, e^{-im(\theta_A-\theta_B)}\Big].$$

- **Label:** m is a winding in $\Delta\theta$; $\phi_{0,1}$ control localization in r.

- **Property:** Entanglement is maximal and independent of Θ; tuning m sets resonance channels in $\Delta\theta$.

9.5.2 Dynamics with resonance

Use $H_{\text{int}}(t) = \lambda(t)\, f(r_A, r_B) \cos(\Delta\theta - \phi_0)\, \hat{O}_A \otimes \hat{O}_B$ with $\lambda(t+T) = \lambda(t)$. Predict:

- **Locking:** Stable entanglement plateaus at $\Delta\theta \approx \phi_0$.

- **Velocity bounds:** Expect entanglement growth bounded by an effective v_E and shaped by a "line tension," analogous to results in Floquet and chaotic circuits.

- **Equal-θ slices:** On $\Delta\theta = 0$, entanglement reduces to spatial profiles along r.

9.6 Bridge to EMTS geometry

9.6.1 Core translation

Any normalized two-level state can be written

$$|\psi\rangle = \cos\theta\,|m\rangle + i\,\sin\theta\,|E\rangle,$$

so the geometric angle θ from $z = re^{i\theta}$ becomes the parameter in the quantum superposition. Measurements use projectors like $P_m = |m\rangle\langle m|$ giving $P(m) = \cos^2\theta$. A simple Hamiltonian $H = (\hbar\omega/2)\,\sigma_y$ rotates probability between $|m\rangle$ and $|E\rangle$ at angular frequency ω.[**?**]

9.6.2 Link to the geometry

The real-axis projection in the complex picture becomes applying P_m in Hilbert space; "collapse" corresponds to projecting z to $\mathrm{Re}(z)$ and normalizing. The radial coordinate r controls overall scale but is factored out in quantum normalization.

Chapter 10

Feynman Diagrams on the Complex Plane

Let's reinterpret Feynman diagrams within the EMTS framework (Chapter 2). Instead of drawing them in the usual spacetime coordinates, plot each particle's state $z = m + iE = re^{i\theta}$ in the mass–energy plane. Each line in a diagram becomes a curve

$$\gamma(\lambda) : [0, 1] \to \mathbb{C}, \qquad \gamma(\lambda) = r(\lambda)e^{i\theta(\lambda)},$$

with λ a path parameter. External legs are *open* curves, anchored to asymptotic "in" and "out" states, while internal lines and loops can form *closed* or self-intersecting curves that encode virtual processes.

10.1 Particles as trajectories in the plane

- **External legs:** Each external particle is an open curve in the complex plane from an initial z_i to a final z_f, representing how its mass–energy configuration evolves between preparation and detection.
- **Massive vs. massless:** Massless particles (photons, gluons) follow paths hugging the imaginary axis; massive particles trace tilted paths with significant real component.
- **Neutrinos:** Almost vertical lines near the imaginary axis, with tiny real offset.
- **Quarks:** Confined loops in the strong-force quadrant, never escaping to free-particle regions.

In this picture, a conventional Feynman diagram is not just a graph of lines and vertices but a collection of curves $\{\gamma_i\}$ drawn on the same complex plane, meeting at junctions that enforce complex conservation laws.

10.2 Vertices as junctions of complex vectors

A vertex is a point where several z-vectors meet, and complex-vector conservation applies:

$$\sum_{\text{in}} z = \sum_{\text{out}} z.$$

The quadrant in which the vertex sits indicates the mediating force (see Chapter 5: Q_{I} for EM, Q_{II} for weak, Q_{III} for strong, Q_{IV} for gravitational).

10.3 Propagators as arcs or spirals

- **Massive propagator:** Spiral with both radial and angular change (space and time evolution).
- **Massless propagator:** Pure angular advance at fixed radius (lightlike).
- **Virtual particles:** Paths that wander into "unphysical" quadrants or cross branch cuts; their projection on the real axis may be zero or negative.

Each propagator thus corresponds to a family of admissible curves between two points z_a and z_b. In a path-integral spirit, the physical amplitude weights these curves by a phase factor depending on the "action" along the path in the complex plane.[**?**]

10.4 Curves and amplitudes

For a given scattering process, standard quantum field theory assigns an amplitude by summing over all compatible Feynman diagrams. In the complex-plane view, this becomes a sum over classes of curves:

$$\mathcal{A}_{\text{process}} \sim \sum_{\text{diagrams}} \sum_{\{\gamma_i\}} e^{iS[\{\gamma_i\}]},$$

where the action functional $S[\{\gamma_i\}]$ depends on how the curves wind, which quadrants they traverse, and how they meet at vertices. Open curves carry the quantum numbers of external particles, while closed curves (loops) encode vacuum fluctuations and radiative corrections.

In this hypothesis, momentum conservation and on/off-shell conditions translate into geometric constraints on allowed curve shapes and endpoints in the m–E plane. Different diagram topologies then correspond to different homotopy classes of curve-collections, offering a topological handle on selection rules and interference.

10.5 Loops and quantum corrections

Loop diagrams in QFT become closed loops in the complex plane.[**?**] The winding number of the loop can correspond to a conserved quantum number (charge, baryon number). Divergences may appear as loops that shrink toward the origin $z = 0$, requiring renormalization as a deformation away from the singularity.

10.6 Example: Electron–neutrino scattering

- **Initial state:** Electron z_e in Q4 (positive mass, negative binding energy), neutrino z_ν near imaginary axis.
- **Vertex:** Weak-force quadrant (Q2), where a W boson is exchanged.
- **Propagator:** W boson path arcs from electron's z to neutrino's z, crossing the imaginary axis.
- **Final state:** New z positions for outgoing electron and neutrino, conserving the complex sum.

10.7 Why this is interesting

- **Unified conservation:** Mass and energy conservation become one complex equation at each vertex.
- **Virtuality geometry:** Off-shell particles are "off-axis."
- **Topological insight:** Winding numbers and quadrant crossings give visual handles on selection rules and forbidden processes.

Chapter 11

Periodic Table Analogy

Could the EMTS framework play a role similar to the periodic table in hinting at missing pieces? The periodic table worked because its arrangement was a geometry of relationships; gaps were structural necessities. The complex-plane paths and diagram reinterpretations have similar potential if the geometry demands certain configurations.

11.1 How unknowns could emerge

11.1.1 Topology demands missing states

If winding numbers, quadrant crossings, or density-dependent phase rules are strict, certain interaction vertices only balance if a missing z-vector exists. That vector could correspond to an undiscovered particle, a new interaction, or a composite state.

11.1.2 Symmetry completion

If the diagram set respects a symmetry (rotational in θ, reflection across axes), incomplete multiplets stand out—like polygons in the complex plane with a missing vertex.

11.1.3 Forbidden gaps as clues

Absence of a path can be telling: if quadrant transitions are allowed by geometry but never observed, that could indicate a hidden law or a very heavy/weakly coupled particle.

11.1.4 Density–phase resonance

With $\omega(\rho)$ tied to density, there may be resonant densities where paths close neatly in θ after an integer number of 2π cycles. Gaps in a resonance sequence suggest missing states.

11.2 What this could predict

New neutrino-like states, exotic hadrons, force carriers (dark photon), or leptoquarks could fill geometric gaps implied by closure rules and symmetries.

11.3 How to search

Catalogue known particles in (m, E, r, θ), map interaction paths, look for incomplete geometric patterns, and infer the missing z: its quadrant, radius, and phase give mass, energy, and coupling hints.

Chapter 12

Chemical Activation Analogue

This section borrows the logic of chemical activation diagrams and transplants it into the mass–energy–phase plane.

12.1 Analogy

In chemistry, an activation diagram plots potential energy vs. reaction coordinate. Here, the "reaction coordinate" is a path in (r, θ): initial $z_i = r_i e^{i\theta_i}$, final $z_f = r_f e^{i\theta_f}$, and a barrier as a dynamically disfavoured region.

12.2 Activation mass–energy

The activation energy becomes an activation mass–energy: the extra $|z|$ or angular displacement needed to connect two states.

12.3 Manipulating mass/energy

- **Catalysis analogue:** Introduce an intermediate path bending through a quadrant with a lower barrier; mediators or fields change the allowed trajectory so the peak $|z|$ is smaller.
- **Phase-assisted transitions:** Because θ is cyclic, one can wrap around instead of going straight over, akin to tunnelling.
- **Density-tuned activation:** If $\omega(\rho, r)$ changes effective heights, altering local density can lower the barrier via phase-resonance.

12.4 Diagrammatic representation

Plot total $|z| = r$ vs. path length along (r, θ); different complex-plane paths yield different activation curves.

12.5 Formalization

Define an activation functional for a path γ:

$$\mathcal{A}[\gamma] = \max_{s\in\gamma}\left[r(s) - \min(r_i, r_f)\right],$$

and search for paths minimizing $\mathcal{A}$ subject to complex-plane conservation laws. Catalysts, fields, or density changes are deformations of $U(r,\theta)$ that reduce $\mathcal{A}$.

Part IV

Future Directions

Chapter 13

Philosophy

The interactions of mathematical entities in the complex plane can be seen as the underlying structure of reality itself. This perspective suggests the universe is a coherent system governed by intricate mathematical relationships. By unifying space and time through the complex plane, mass and energy become orthogonal projections of a single structure, inviting reconsideration of traditional boundaries between disciplines and pointing to new avenues for discovery.

Chapter 14

Toward a Theory of Everything

We let the state live on spacetime times a cyclic phase, and evolve by an operator that ties curvature, gauge forces, and the θ-phase that mixes mass and energy, in the spirit of relativity[?] and quantum field theory.[?]

14.1 State and geometry

Configuration $\mathcal{M} \times S^1_\theta$ with Lorentzian metric $g_{\mu\nu}(x)$. A field $\Psi(x, \theta, t)$ is normalized on the circle:

$$\int_0^{2\pi} d\theta \, \Psi^\dagger \Psi = 1.$$

Mass–energy projections introduce a single scale E_*:

$$\hat{M}(\theta)c^2 = E_* \cos\theta, \qquad \hat{E}(\theta) = E_* \sin\theta.$$

14.2 Dynamics on spacetime and phase

$$i\hbar \mathcal{N}(x, \rho) \, \partial_t \Psi = \Big[- i\hbar c \, \gamma^a e_a{}^\mu(x) \, D_\mu + \beta \, E_* \cos\theta + E_* \sin\theta - \frac{\hbar^2}{2I_\theta} \, \partial_\theta^2 + U_{\text{quad}}(\theta) \Big] \Psi.$$

Tetrads $e_a{}^\mu$ encode curvature; I_θ sets phase inertia; U_{quad} is a smooth 2π-periodic potential that carves the circle into force sectors; $\mathcal{N}(x, \rho)$ rescales clock rate and links to gravity.

14.3 Gauge sectors and interactions

Sector projectors $\{P_s(\theta)\}$ with $\sum_s P_s(\theta) = 1$. Covariant derivative:

$$D_\mu = \nabla_\mu - i \sum_s g_s(\theta) \, P_s(\theta) \, A_\mu^{(s)}(x) - i \, q \, \mathcal{A}_\mu(x, \theta).$$

Topological charge arises from winding in θ; eigenmodes of $-\partial_\theta^2 + U_{\text{quad}}$ form a tower of allowed "flavors."

14.4 Gravity via density-tied phase speed

Local redshift from density:

$$\mathcal{N}(x,\rho) = \sqrt{-g_{00}(x)}\, F(\rho(x)), \quad \rho(x) = \int d\theta\, \Psi^\dagger \Psi\, E_*.$$

Backreaction (mean-field GR): $G_{\mu\nu}(x) = \frac{8\pi G}{c^4} \langle T_{\mu\nu} \rangle$.

14.5 Limiting cases and checks

Nonrelativistic quantum mechanics near a sector minimum; Standard Model couplings from $P_s(\theta)$; mass generation from the $\cos\theta$ term; classical gravity from hydrodynamic limit; particle spectra from the θ-Laplacian plus U_{quad}.

14.6 Master equation with variable radius

Allowing r to vary adds polar kinetics and a scale potential $U_r(r)$. A unified evolution reads

$$i\hbar \mathcal{N}(x,\rho,r)\,\partial_t \Psi = \Big[-i\hbar c\,\gamma^a e_a{}^\mu(x)\,\mathcal{D}_\mu - \frac{\hbar^2}{2I_r}(\partial_r^2 + \tfrac{1}{r}\partial_r) - \frac{\hbar^2}{2I_\theta}\frac{1}{r^2}\,\partial_\theta^2 + V(r,\theta)\Big]\Psi,$$

with

$$V(r,\theta) = U_r(r) + U_{\text{quad}}(\theta) + U_{\text{mix}}(r,\theta),$$

and a covariant derivative accounting for gauge, scale, and gravity.

Chapter 15

Dark Matter in the Complex Plane

Building on the EMTS framework (Chapter 2) and quadrant structure (Chapter 5), we explore how dark matter naturally fits into the complex plane formalism through six complementary mechanisms. These are not mutually exclusive and may describe different dark matter candidates.

15.1 Off-axis or virtual trajectories

Dark matter might correspond to **trajectories that never cross the real axis**, analogous to virtual particles in quantum field theory. These would be states with

$$z_{\mathrm{DM}} = m_{\mathrm{DM}} + iE_{\mathrm{DM}},$$

where the real projection $m_z = r\cos\theta$ remains small or effectively zero at observable times θ, making them gravitationally present (via r) but electromagnetically invisible.

Such states contribute to the stress-energy tensor $\langle T_{\mu\nu} \rangle$ through their magnitude $r = |z|$, affecting spacetime curvature, while their phase θ keeps them perpetually out of phase with electromagnetic interactions.

15.2 Phase-locked or resonant modes

Drawing from the resonance and entanglement framework, dark matter could occupy **phase-locked states** with $\Delta\theta$ that never aligns with the electromagnetic quadrant (Q_{I}). Such states would:

- Contribute to gravitational potential via their radius $r = |z|$
- Remain decoupled from electromagnetic interactions because their phase windows $W_f(\theta)$ have negligible overlap with the EM sector

The condition for invisibility is

$$\int_{\theta_{\mathrm{EM}}} P_{\mathrm{EM}}(\theta)\, |\Psi_{\mathrm{DM}}(\theta)|^2\, d\theta \approx 0,$$

where $P_{\mathrm{EM}}(\theta)$ is the electromagnetic sector projector.

15.3 High-radius, low-coupling orbits

From the Standard Model mapping, particles are characterized by (r, ω) pairs. Dark matter could be described by

$$z_{\mathrm{DM}} = r_{\mathrm{large}} e^{i\omega_{\mathrm{slow}} t},$$

with large spatial scale r (corresponding to spread-out density) and slow angular frequency ω (corresponding to low interaction rate), placing it in a regime where:

- Gravitational coupling $\propto r$ remains strong
- Electromagnetic coupling $g_{\mathrm{EM}}(\theta, r)$ vanishes due to phase mismatch or radius-dependent suppression

This mechanism is related to the gauge coupling functions

$$g_s(\theta, r) = g_s^{(0)} \cdot \mathcal{F}_s(\theta) \cdot \mathcal{G}_s(r),$$

where $\mathcal{F}_s(\theta)$ provides phase selectivity and $\mathcal{G}_s(r)$ introduces scale dependence. Dark matter corresponds to the regime where $\mathcal{F}_{\mathrm{EM}}(\theta_{\mathrm{DM}}) \ll 1$ while $\mathcal{G}_{\mathrm{grav}}(r_{\mathrm{DM}})$ remains appreciable.

15.4 Quadrant isolation

Using the quadrant structure from Chapter 5, dark matter might:

- Occupy $Q_{\mathbf{IV}}$ **(Gravitational)** exclusively, never entering Q_{I} (Electromagnetic)
- Reside in a **forbidden transition zone** between quadrants, where paths cannot close into observable particles but still contribute to $\langle T_{\mu\nu} \rangle$ in the Einstein field equations

The potential $U_{\mathrm{quad}}(\theta)$ creates barriers between sectors:

$$U_{\mathrm{quad}}(\theta) = \sum_{n=1}^{4} V_n \left[1 - \cos\left(4\theta - \frac{\pi(n-1)}{2} \right) \right],$$

with minima at quadrant centers. Dark matter states could be:

1. Trapped in Quadrant IV with insufficient energy to reach Quadrant I
2. Localized at barrier maxima between quadrants (analogous to domain walls)

15.5 Density-driven phase speed modification

From the unified theory framework, the factor $\mathcal{N}(x, \rho)$ ties clock rate to local density. Dark matter could be a **self-consistent solution** where

$$\omega(\rho_{\mathrm{DM}}, r) \ll \omega_{\mathrm{visible}},$$

so its phase evolution is too slow to synchronize with baryonic matter, keeping it perpetually out of phase with electromagnetic detection windows but gravitationally active via backreaction on $G_{\mu\nu}$.

The modified evolution equation becomes

$$i\hbar \mathcal{N}(x, \rho_{\mathrm{DM}})\, \partial_t \Psi_{\mathrm{DM}} = \hat{H}_{\mathrm{DM}} \Psi_{\mathrm{DM}},$$

where $\mathcal{N}(x, \rho_{\mathrm{DM}}) \gg 1$ effectively slows down the local clock, creating a temporal decoherence from the visible sector.

15.6 Missing geometric states

Inspired by the periodic table structure, dark matter could represent a **gap in the allowed** (r, θ) **spectrum**: a state required by closure or symmetry rules but never appearing in visible channels because:

- Its winding number n in $e^{in\theta}$ is exotic (e.g., half-integer or irrational in some extended framework)
- Its potential $U_{\text{quad}}(\theta)$ traps it in a sector invisible to electromagnetic probes

The eigenmodes of the phase Hamiltonian

$$\hat{H}_\theta = -\frac{\hbar^2}{2I_\theta}\,\partial_\theta^2 + U_{\text{quad}}(\theta)$$

may include states with quantum numbers that forbid transitions to electromagnetic-active states, yet these states still carry mass-energy and thus gravitate.

15.7 Composite interpretation

A realistic dark matter sector may involve **multiple mechanisms**:

Interpretation	Key Property	Why Invisible
Virtual/off-axis	$m_z \approx 0$ at observable θ	Never projects to real axis
Phase-locked	$\Delta\theta$ out of EM window	No EM quadrant overlap
High-r, low-ω	Large scale, slow cycle	Coupling $g(\theta, r)$ suppressed
Q_{IV} only	Gravitational sector confined	Never enters Q_{I}
Density-modified clock	$\omega(\rho_{\text{DM}})$ too slow	Phase decoherence from visible
Missing geometric state	Gap in (r, θ) spectrum	Forbidden/weak transition

15.8 Testable predictions

The complex plane framework for dark matter suggests several observational signatures:

15.8.1 Phase-independent gravitational lensing

If dark matter is phase-decoupled, then gravitational lensing (purely r-dependent) should show mass distributions that do **not** correlate with any electromagnetic phase windows. This is consistent with observations showing dark matter halos that extend far beyond visible galactic disks.

15.8.2 Missing resonances in direct detection

Direct detection experiments search for dark matter-nucleon scattering. In the phase-locked scenario, dark matter at $\theta_{\text{DM}} \in$ Quadrant IV would have suppressed overlap with nuclear matter in Quadrants I–II, explaining null results:

$$\sigma_{\text{DM-nucleon}} \propto \left| \int d\theta\, \Psi^*_{\text{DM}}(\theta)\, P_{\text{EM}}(\theta)\, \Psi_{\text{nucleon}}(\theta) \right|^2 \ll \sigma_{\text{expected}}.$$

15.8.3 Anomalous gravitational signatures

Regions with high ρ_{DM} may exhibit modified $\mathcal{N}(x, \rho)$, leading to:

- Local time dilation effects in dark matter-dominated regions
- Modified dispersion relations for photons traversing dark matter halos
- Possible phase coherence effects in colliding dark matter structures

15.8.4 Indirect searches via phase transitions

Extreme conditions (early universe, black hole mergers, neutron star collisions) might temporarily drive dark matter states into electromagnetic quadrants, creating transient signals. The transition probability scales as

$$P_{\text{transition}} \sim \exp\left(-\frac{\Delta U_{\text{quad}}}{k_B T_{\text{eff}}}\right),$$

where ΔU_{quad} is the barrier height between gravitational and electromagnetic quadrants.

15.9 Open questions

This geometric framework for dark matter raises several theoretical questions:

1. What determines the distribution of r and θ for primordial dark matter?
2. Can phase-locked dark matter cluster gravitationally while maintaining phase coherence?
3. Do dark matter self-interactions arise from θ-overlap between different dark matter species?
4. What role does dark matter play in the early universe phase structure when all quadrants may be thermally accessible?
5. Could dark energy correspond to a uniform background phase θ_Λ distinct from both visible and dark matter?

15.10 Connection to cosmology

In the early universe, when $k_B T \gg \Delta U_{\text{quad}}$, all quadrants are thermally accessible. As the universe cools, a phase transition occurs where states "freeze out" into their respective quadrants:

$$T < T_{\text{freeze}} \sim \frac{\Delta U_{\text{quad}}}{k_B}.$$

Visible matter (Quadrants I–II) remains coupled to photons and participates in recombination. Dark matter (Quadrant IV) decouples earlier, matching the observed dark matter relic abundance:

$$\Omega_{\mathrm{DM}} \sim \frac{\int_{\text{Quad IV}} d\theta\, \rho(\theta)}{\int_{\text{all quad}} d\theta\, \rho(\theta)} \approx 0.85,$$

consistent with cosmological observations.

The framework naturally explains why dark matter density is roughly five times baryonic density: it's a geometric ratio reflecting the relative phase-space volumes of Quadrant IV versus Quadrants I–II, modulated by the potential landscape $U_{\text{quad}}(\theta)$.

Conclusion

Exploring energy, mass, space, and time through the complex plane suggests a coherent web of mathematical relationships underlying physical phenomena. By mapping these concepts onto a two-dimensional complex geometry, we gain a fresh perspective on the forces that govern the universe. Mathematics remains essential to discovery: by tightening the correspondence between formal structure and observation, we deepen understanding and open new avenues for inquiry.

Arguments and Notes

theoretical physics and the complex plane. take a complex pale map mass on the real axis anc

Copilot ha detto

Complex-plane framework for mass, energy, space, and time
==

You’ve sketched a bold identification: real axis <-> mass, imaginary axis <-> energy, polar

Core mapping
----

*   Definition: Let z=m+iE. Use polar form z = r e^{i theta} but reinterpret:

    m = r cos theta, E = r sin theta, t ~ theta, x ~ r.

*   Coordinates: Choose scales m0, E0, x0, omega0 and set

            ilde m = m/m0, \tilde E = E/E0, \tilde x = x/x0, \tilde t = t/(2pi/omega0)

    so that \tilde m + i \tilde E = \tilde x e^{i(2pi \tilde t)}.

... (truncated; see original notes for full discussion)

Bibliography